Engineering Failure Analysis 146 (2023) 107077

Contents lists available at ScienceDirect

Engineering Failure Analysis

journal homepage: www.elsevier.com/locate/engfailanal

Ultrasound-based structural health monitoring methodology employing active and passive techniques

Josu Etxaniz [a,*], Gerardo Aranguren [a], José Miguel Gil-García [b], Jesús Sánchez [b], Gabriel Vivas [a], Jon González [a]

[a] *Faculty of Engineering, University of the Basque Country (UPV/EHU), 48013 Bilbao, Spain*
[b] *Faculty of Engineering, University of the Basque Country (UPV/EHU), 01006 Vitoria-Gasteiz, Spain*

ARTICLE INFO

Keywords:
Structural Health Monitoring (SHM)
Ultrasound active test
Ultrasound passive test

ABSTRACT

Currently, structures are examined during manufacturing by means of Non Destructive Tests (NDT), but there is an increasing interest in monitoring its integrity over its whole life cycle by using Structural Health Monitoring (SHM) strategies. The monitoring of aircraft structures is particularly important as they suffer high strain under extreme atmospheric conditions. There is an extensive literature on SHM for aviation available but there are few references on comprehensive methodologies. This article introduces a methodology, a device and the tests used in its validation. The electronic prototype for structural health monitoring applies ultrasound techniques by means of piezoelectric transducers. It is lightweight, has USB 2.0 connectivity and includes data pre-processing algorithms to improve its performance. It can run in pitch-catch and pulse-echo modes employing passive and active techniques. Passive techniques are used to detect impacts or fiber breakage in composite materials. Tests based on active techniques can bring to light several types of damages such as those caused abruptly or those produced progressively by corrosion, delamination or fatigue.

1. Introduction

Impacts can weaken structures critically. The severity of the damage caused depends on the velocity, location, and energy of the sources of impacts [1]. In the case of aeronautical structures, such sources usually are hail, meteors, or birds. No structure is free from impacts, i.e. unwanted and uncontrolled bumps. Apart from impacts, there are some other phenomena that weaken structures, namely, manufacturing flaws, scratching, ageing, or corrosion. The main risk of such sort of damage in structures is that it could be invisible, particularly in composite structures when the damage is internal, such as fiber breakage. As a result, the usually important cost of visual maintenance inspection, known as Visual Testing (VT), sometimes could be just a waste of time and money. The most common methods in composite Non Destructive testing (NDT) applications are VT, Ultrasonic Testing (UT), Thermography, Radiographic Testing, Electromagnetic Testing, Acoustic Emission (AE), and Shearography Testing [2]. The aim is to apply NDT techniques along aircraft lifespan, according to Structural Health Monitoring (SHM) techniques [3].

One of the hottest research topic that attracts interest from academia and industry is how to know the health state of any structure over its lifespan. For instance, Capineri and Bulleti introduced a comprehensive review of the state-of-the-art in SHM, from the

---

* Corresponding author.
E-mail address: josu.etxaniz@ehu.es (J. Etxaniz).

https://doi.org/10.1016/j.engfailanal.2023.107077
Received 23 February 2022; Received in revised form 22 November 2022; Accepted 16 January 2023

characterization of the signals to the main monitoring techniques [4].

Structures can be monitored by using sensors that suffer the damage simultaneously with the structure (direct sensing) [5]: fibers, strain gauges, etc. Unfortunately, the success of these techniques is limited by the location of the sensors along the structure. On the other hand, structures can be monitored by using themselves as a means to transmit its health state (indirect sensing) using eddy currents [6], ultrasound waves [7], or vibrations [8]. Indirect sensing methods are more effective and easier to implement than direct sensing methods.

This paper focuses on ultrasound methods, which are gaining significance. They are based on piezoelectric wafer active sensors (PWAS) [9]. A PWAS transforms electric signals into acoustic waves that propagates over the material and vice versa. The low cost and mounting simplicity of PWAS sensors allow envisaging its generalized deployment in aeronautics in the near future.

Typically, an SHM Ultrasound System (SHMUS) and several PWASs are necessary to monitor the health of a structure. An SHMUS is the electronic system that handles the PWASs attached and/or embedded to the structure under test. If the structure is complex, as some of those included in an aircraft or a ship, a network of SHMUSs is mandatory.

Ultrasound methods operate with PWAS in two modes: passive or Acoustic Emission (AE) mode and active or Ultrasound Guided Wave Test (UGWT) mode [10]. In AE, SHMUS is continuously acquiring and processing the signals read by the PWASs [11]. It tries to discover any change in the signals compatible with an impact in the structure or a fiber breakage in a composite-made structure [12]. Conversely, when operating UGWT, SHMUS generates driving signals that are coupled to the structure through the PWASs. They produce waves that propagate along the structure and interact with its elements, bouncing back to the very same PWASs, where they can be read back and processed to determine the health state of the structure [7,13].

After the acquisition of waveforms in the set of PWASs, the signals are processed to extract meaningful and comprehensible information about the state of the structure. Azuara et al. introduces a thorough review of the algorithms available to process the signals acquired [14].

There are many publications regarding signal processing in UGWT. They are usually focused on particular cases, with specific impact sources, over laboratory-oriented structures, with suitable sensors, and introducing algorithms, which only seek foreseeable damage.

This paper focuses on describing the methodology and equipment for health-state determination of a structure that suffers from various types of damage. Two types of damage are considered: time-based damage, as corrosion [15], fatigue [16], or delamination [17], and damage due to an abrupt event, such as impacts, fiber breakages in composite material, or operation failures [1,18]. The monitoring of progressive damage using ultrasounds in a structure requires testing the structure over an interval of time with active techniques [19]. However, a sudden damage can be assessed listening to AE.

During the research introduced in this paper, an electronic equipment was developed, more specifically, an SHMUS. This tool combines AE and UGWT techniques or operation modes. Both techniques were validated in a laboratory test campaign.

The remainder of the paper is organized as follows. Section 2, Materials, introduces the developed SHMUS prototype and the specimens under test considered. Section 3 describes the methodology of operation that supports the test performed in the research. Section 4, Results and Discussion, is divided into two subsections that gives details about how sudden damage and progressive damage is determined by SHMUS. Section 5 provides concluding remarks and suggests future works.

2. Materials

According to most of the experimental literature, the most common choice for the instrumentation to consider in ultrasound based SHM researches is the commercial one, i.e. arbitrary signal generators and oscilloscopes. For instance, Mei et al. [9] published a comprehensive analysis and setup for PWAS based SHM, where they describe how to utilize commercial instrumentation. Generic IO systems can be found as instrumentation for ultrasound based SHM in other literature [20]. However, the driving signal generation in UGWT, the number of available sensors, and the monitoring techniques offered by such electronic systems and instrumentation are very limited.

On the other hand, some dedicated instrumentation can also be found. For example, a standalone two-channel AE system to monitor pressure slow-speed bearings, pipelines, vessels, and other machinery [21], a highly integrated CMOS transceiver capable of transmitting and acquiring a signal for UGWT [22], or a set of devices to actively and passively monitor several types of structures [23]. Furthermore, Dattoma et al. used some ultrasonic devices to know the health state of a certain structure during its production or for maintenance purposes [24]. Sharif-Khodaei et al. developed a platform to measure the wave propagation impedance with passive sensing, active sensing, and optimal sensor positioning methods [25]. Unfortunately, usually they are not the best choice for real-world monitoring tasks as long as they require an operator or they are big and/or expensive enough to make them viable to be permanently installed in a structure.

The typical requirements for instrumentation that applies AE and UGWT techniques are well-known features. On the one hand, AE technique demands a very high number of PWASs per structure, usually in the range from 10 to 50. A trigger is also mandatory for such instrumentation, a trigger similar to those in each channel included in oscilloscopes. On the other hand, a groundbreaking feature in UGWT is the capability to drive a set of PWASs, typically from 5 to 20 units, with adjustable delay signals, in the range of just a few nanoseconds. The signal generator limits the amplitude of the PWASs driving signals, usually in the range of 10 to 20 Vpp. The results of UGWT on metallic structures demonstrate that such range of amplitude of driving signals is enough for them to be satisfactory. However, higher amplitudes, which can be up to 100 Vpp, are necessary on composite structures. Finally, a real-world monitoring tool must be small and lightweight to be usable embedded in aircrafts. It must operate with no human interaction and transmit the monitoring information to a control central node autonomously.

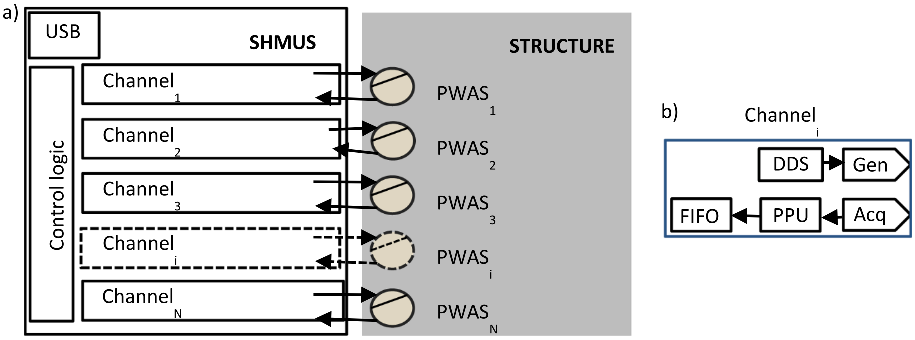

Fig. 1. Block diagram of the current version of the self-developed SHMUS, a) SHMUS and structure under test, b) detail of the blocks inside each channel.

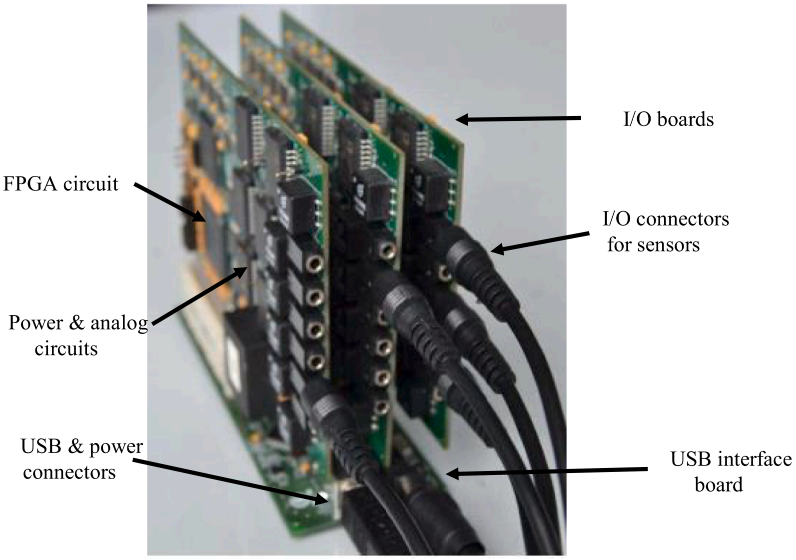

Fig. 2. SHMUS modular system fitted with three input/output cards capable to drive and acquire 18 signals.

The Electronic Design Group of the University of The Basque Country (UPV/EHU) has developed several SHMUS that implements AE and UGWT techniques. The previous version [26] is based on Virtex 5 Field Programmable Gate Array (FPGA) with a PowerPC processor running Linux. The ever-growing demand for new processors and up-to-date operating systems motivated the development of a new version. The current version of SHMUS is a modular system that consists of an USB interface and from one to eight input/output electronic cards, which feature an FPGA of the Xilinx Artix 7 family. More specifically, the current version includes the XC7A50T FPGA, which contains more than 50,000 logic cells. Furthermore, the FPGA needs no support of firmware or embedded processor to avoid the issue of deprecation of electronic systems due to the obsolescence of the operating systems or the embedded firmware. The software to control the monitoring tool runs in an external computer.

Fig. 1**a** shows the block diagram of the self-developed SHMUS connected to a set of PWASs glued to the structure under test. The main blocks of SHMUS are the control logic module, the channels to excite and acquire signals from the transducers, and the USB connectivity block. The commands from the control software reach SHMUS through the USB block. Similarly, the data acquired go through the same block from SHMUS to the control software. The control logic module manages the performance of the channels, and the channels provide and acquire the acoustic waveforms to monitor the state of the structure. Each channel is composed of the generation and the acquisition circuits (see Fig. 1b). The generation circuit contains the Direct Digital Synthesis block (DDS), which generates the waveforms and it is implemented inside the FPGA; and the analog Generation block (Gen), which adapts the amplitude of the waveform to be given to the PWAS. The acquisition circuit is divided into the signal analog acquisition block (Acq), the pre-processor unit (PPU), and a FIFO memory. Acq is composed of a conditioning circuit, a low-noise amplifier, a filter, and an analog-to-digital converter. Finally, PPU extracts the maximum and minimum peaks from the received waves, which are stored in the FIFO memory.

Fig. 2 shows an SHMUS prototype that includes three boards. Each board can handle six channels and, therefore, the prototype in the figure can generate and acquire signals for 18 channels at the same time. Each channel can drive a PWAS to emit an excitation

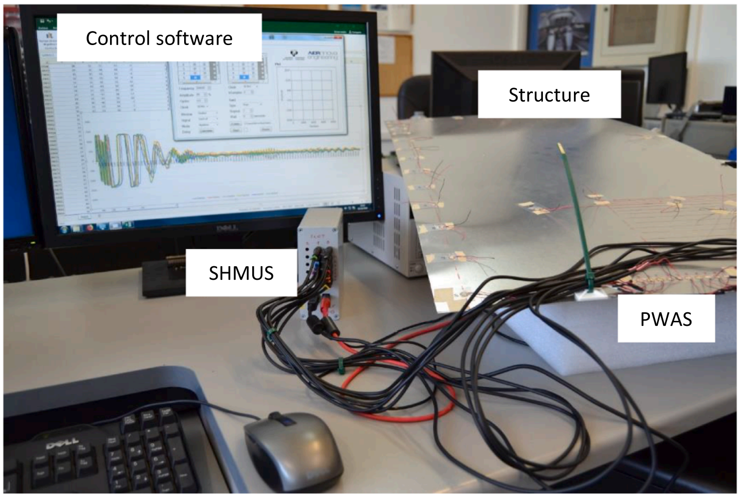

Fig. 3. Photography of the setup of the tests.

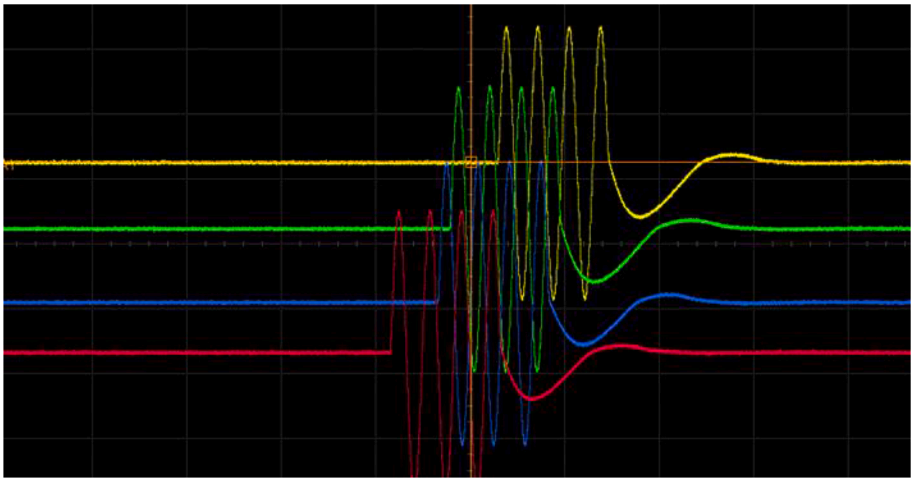

Fig. 4. Screen capture of the oscilloscope acquisition in the leads of four PWASs when 300 kHz waveform is applied (deflection factors 10 V/div and time base 5 μs/div). SHMUS output is configured with adjustable delays. The capture shows delays adjusted to 5.23 μs, 6.57 μs and 11.67 μs.

signal. Simultaneously, each channel can acquire the excitation signal and the reflected signals after the propagation of signals throughout the structure under test. The prototype in the figure weights 600 gr and its dimensions are 125 × 125 × 50 mm, when it is inside the aluminum box.

To the best of authors' knowledge, literature does not report any other SHM equipment that operates with ultrasound technique and handles more than one signal generator at a time.

3. Method

Fig. 3 shows the setup of the tests of this research. It includes a computer with the software to control the test, an SHMUS, and the structure under test with a set of PWASs permanently attached to the structure. The operating principle is that any damage caused to the structure will modify the propagation of the waves through the structure [7] and, therefore, the signals acquired in the SHMUS.

The system can run either passive or active tests. Passive tests consist of continuously acquiring signals from all enabled channels to detect a trigger condition by processing those signals. This processing is carried out by the FPGA in all channels concurrently. When a trigger condition happens, the signals acquired by all channels are stored from that moment until the FIFO memory is filled.

Active tests consist of generating superficial excitation waveforms that will propagate throughout the structure. Those waveforms get reflected at the edges or irregularities of the structure and acquired back at the PWASs. The active tests can be configured in several ways:

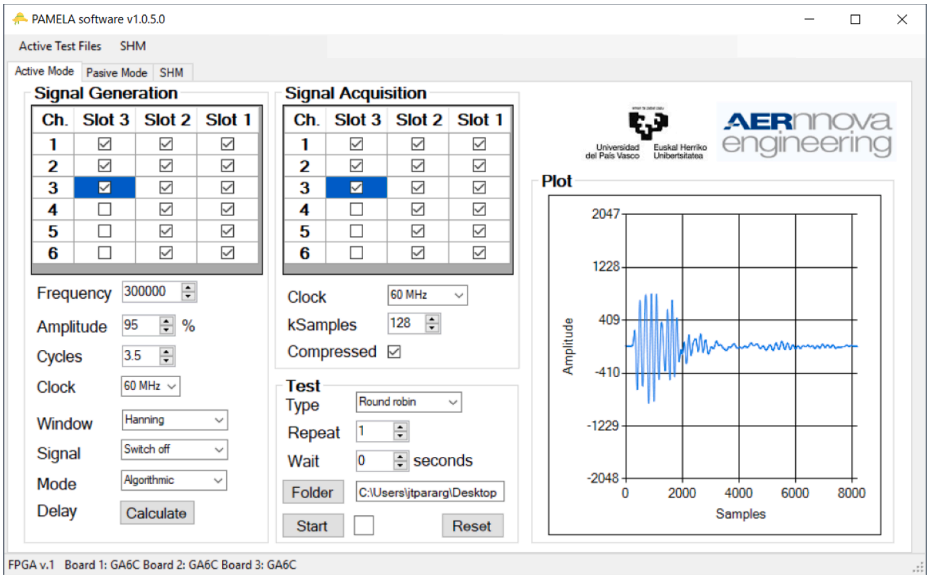

Signal Generation

Ch.	Slot 3	Slot 2	Slot 1
1	☑	☑	☑
2	☑	☑	☑
3	☑	☑	☑
4	☐	☑	☑
5	☐	☑	☑
6	☐	☑	☑

Frequency 300000
Amplitude 95 %
Cycles 3.5
Clock 60 MHz
Window Hanning
Signal Switch off
Mode Algorithmic
Delay

Signal Acquisition

Ch.	Slot 3	Slot 2	Slot 1
1	☑	☑	☑
2	☑	☑	☑
3	☑	☑	☑
4	☐	☑	☑
5	☐	☑	☑
6	☐	☑	☑

Clock 60 MHz
kSamples 128
Compressed ☑

Test
Type Round robin
Repeat 1
Wait 0 seconds
Folder C:\Users\jtpararg\Desktop
Start ☐

FPGA v.1 Board 1: GA6C Board 2: GA6C Board 3: GA6C

Fig. 5. SHMUS control software main window.

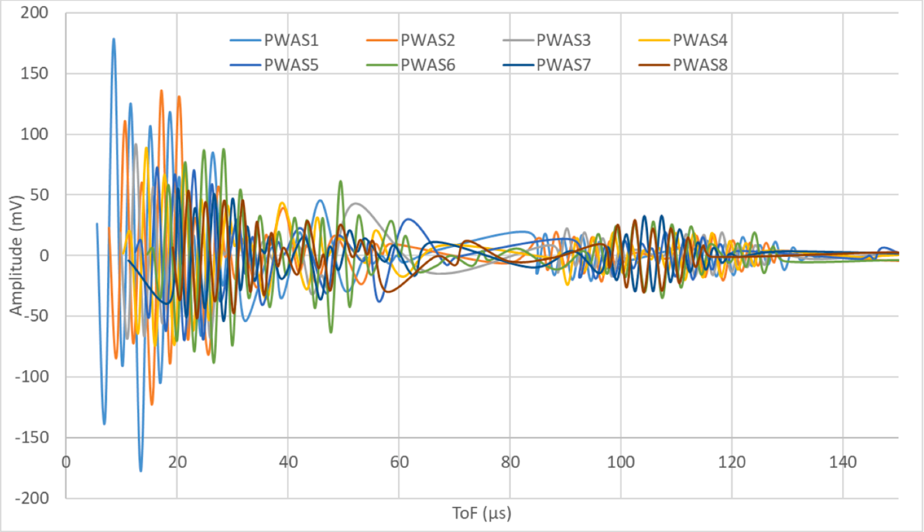

Fig. 6. SHMUS full waveform retrieval of eight signals.

- Simple. Only one single transducer drives the structure while all the enabled PWASs receive the echoes. It is a pitch-and-catch type of test, where as many waveforms as installed PWAS (N) are obtained.
- Round-robin. A Simple test is run for each installed PWAS. Hence, N^2 waveforms are obtained. This test allows using virtual or receiver beamforming [27].
- Transmission beamforming [28]. The amplitude and delay of the driving voltage of each PWAS is generated aiming at the creation of constructive interferences in a given direction. The designed prototype is programmed to sweep from 0° a 180° in steps of 5° obtaining 37 echoes and 37xN waveforms per test.
- Multiple delayed signal. This type of test aims at concentrating the transducers' energy on a given part of the monitored structure. Therefore, the delay of each exciting signal of each PWAS can be arbitrarily configured (Fig. 4).
- Time reversal [29]. This test consists of exciting the PWASs with the waveforms acquired in any of the active tests mentioned above.

Fig. 5 shows the main window of the control software. It shows the selective configuration for both the signal generation and the acquisition channels. "Slot" refers to a board capable of capturing up to six acquisition channels. On the one side, the excitation signal is created inside the FPGA attending at the specifications chosen by the user in the graphical interface: frequency (in the range from 30

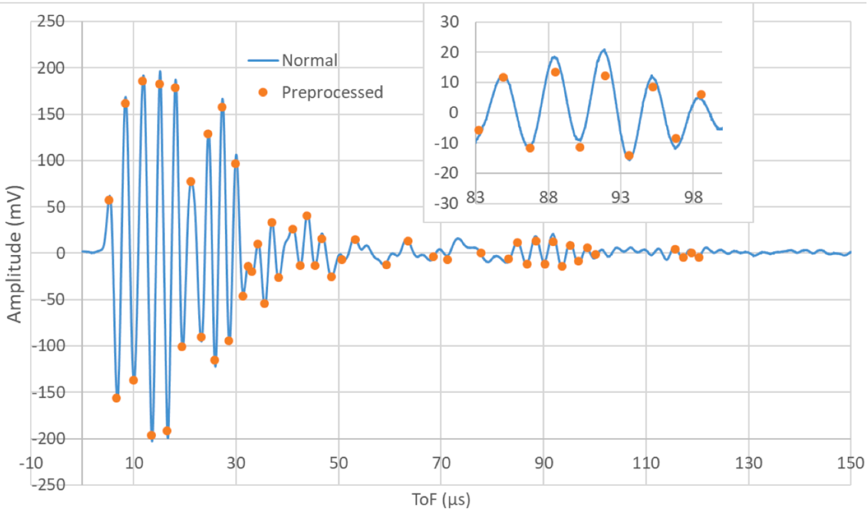

Fig. 7. Full acquisition and compressed acquisition mode comparison on a composite plate.

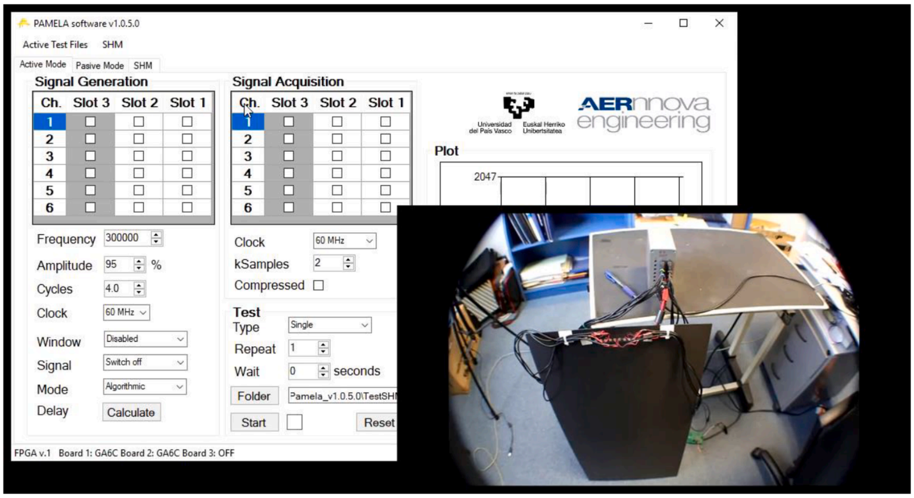

Signal Generation

Ch.	Slot 3	Slot 2	Slot 1
1	☐	☐	☐
2	☐	☐	☐
3	☐	☐	☐
4	☐	☐	☐
5	☐	☐	☐
6	☐	☐	☐

Frequency 300000
Amplitude 95 %
Cycles 4.0
Clock 60 MHz
Window Disabled
Signal Switch off
Mode Algorithmic
Delay

Signal Acquisition

Ch.	Slot 3	Slot 2	Slot 1
1	☐	☐	☐
2	☐	☐	☐
3	☐	☐	☐
4	☐	☐	☐
5	☐	☐	☐
6	☐	☐	☐

Clock 60 MHz
kSamples 2
Compressed ☐

Test
Type Single
Repeat 1
Wait 0 seconds
Folder Pamela_v1.0.5.0\TestSH
Start ☐

FPGA v.1 Board 1: GA6C Board 2: GA6C Board 3: OFF

Fig. 8. Screen capture of the demonstration video of the capabilities of the SHMUS system.

kHz to 1 MHz) amplitude (as a percentage of 48 Vpp), number of periods and its shape (sinusoidal or windowed). It can also synthetize arbitrary waveforms. On the other side, the acquisition unit features a 12-bit resolution where the amount of captured data can be defined along with the sampling frequency (from 10 MHz to 60 MHz).

The acquired signals can be either be fully retrieved (Fig. 6) or they can be processed while they are acquired, looking for maximum and minimum voltages (Fig. 7) which are deemed to be characteristic points of the captured waveform. In this case, a compressed acquisition mode is activated which leads to dramatically decrease the transmission data [30]. Another feature of the developed SHMUS is that the output voltage drops are isolated from each other, which allows achieving exciting voltages higher than 100 Vpp. Fig. 8 shows a screen capture of the demonstration video of the system's capabilities [31].

In order to validate the system, different tests have been carried out on two type of materials, i.e., carbon-fiber reinforced polymer (CFRP) and aluminum as they show different waveform propagation behavior.

The tests can be divided into two types, the ones to detect impacts, and those to detect progressive damages. However, both are based on the propagation of ultrasound acoustic waves.

4. Results and discussion

4.1. Impact detection by means of passive operating mode

The first type of tests are based on the Impact Detection System (IDS) included in SHMUS. Any impact on the structure under test

Fig. 9. Setup to produce controlled impacts on a CFRP board.

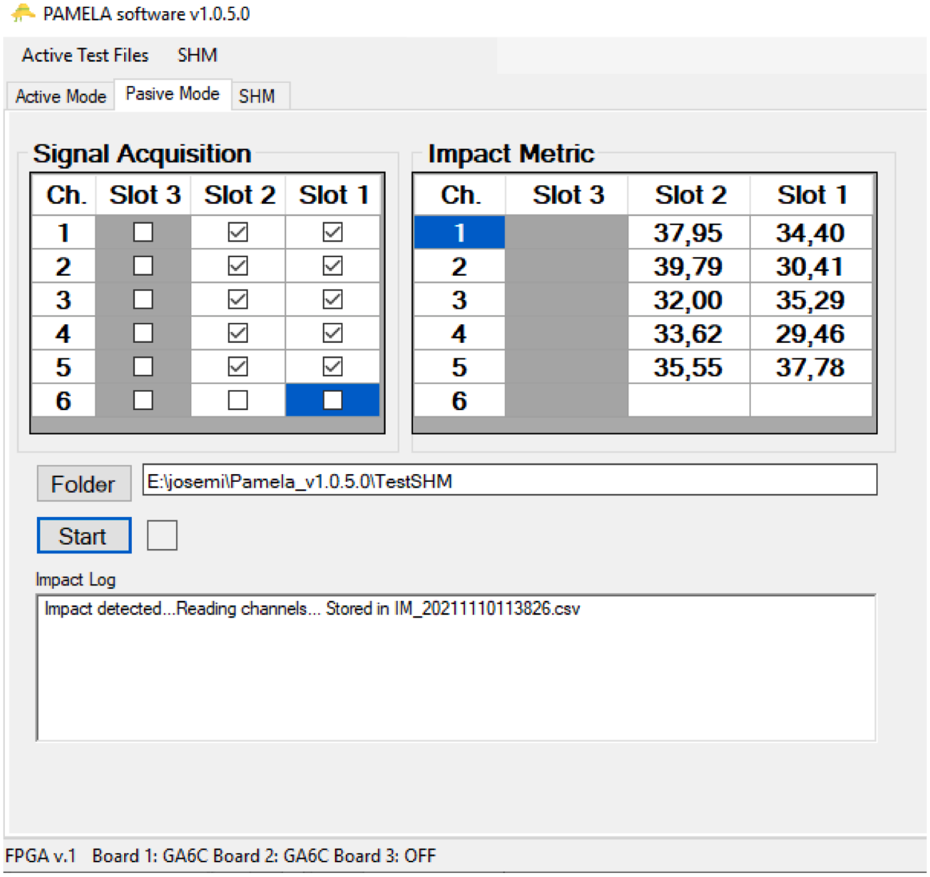

Signal Acquisition

Ch.	Slot 3	Slot 2	Slot 1
1	☐	☑	☑
2	☐	☑	☑
3	☐	☑	☑
4	☐	☑	☑
5	☐	☑	☑
6	☐	☐	☐

Impact Metric

Ch.	Slot 3	Slot 2	Slot 1
1		37,95	34,40
2		39,79	30,41
3		32,00	35,29
4		33,62	29,46
5		35,55	37,78
6			

Folder: E:\josemi\Pamela_v1.0.5.0\TestSHM

```
Impact detected...Reading channels... Stored in IM_20211110113826.csv
```

FPGA v.1 Board 1: GA6C Board 2: GA6C Board 3: OFF

Fig. 10. Control software screen for impact testing (passive mode) that shows several values related to the energy of the detected impact in the Impact Metric section.

generates an acoustic wave that IDS can detect. The parameters of the waveform generated depend on the energy of the impact. As shown in Fig. 9, two elements were necessary to control the energy of a real impact: a 600 g steel ball and a tube with a set of holes at different heights.

If a known mass drops from a known height, a well-known formula provides the impact energy and object velocity. Initially, the

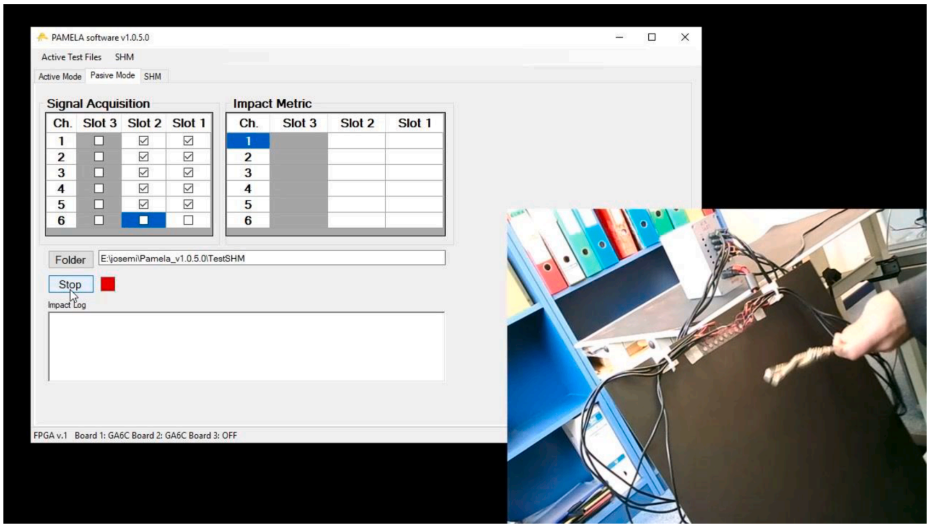

Signal Acquisition

Ch.	Slot 3	Slot 2	Slot 1
1	☐	☑	☑
2	☐	☑	☑
3	☐	☑	☑
4	☐	☑	☑
5	☐	☑	☑
6	☐	☐	☐

Impact Metric

Ch.	Slot 3	Slot 2	Slot 1
1			
2			
3			
4			
5			
6			

E:\josemi\Pamela_v1.0.5.0\TestSHM

FPGA v.1 Board 1: GA6C Board 2: GA6C Board 3: OFF

Fig. 11. Screen capture of the video to show the passive detection system.

impact detection system was tested on two plates, one made of an isotropic material and the other one made of an anisotropic material. Isotropic materials, as metallic materials, show the same mechanical properties along the three axes, while anisotropic materials, as CFRP, do not. Aluminum and CFRP plates with a set of PWASs adhered to them at the edge were utilized in this research.

The purpose is to compare the data obtained from the sensors when applying different energy and different distance from the sensors. Fig. 10 shows the screen of the control software when a passive test to detect an impact is run. On the left side, the operator configures the acquisition channels, which are arranged in two slots in the example shown. A 60 MHz simultaneous acquisition through the selected channels begins when the Start button is pressed. A logic circuit inside the FPGA processes the incoming data (or waveforms) to find when they are over a certain voltage threshold, or to detect a maximum or a minimum inside a range. In the same way as in an oscilloscope, once the logic circuit is triggered, it keeps on processing the waveforms to obtain the maximum and minimum values of the captured signal.

The passive mode test detects the energy and position of an impact. The Impact Metric section in Fig. 10 shows the energy of an impact measured by each configured input channel. In this case, the metric is obtained as the normalized average of the absolute maximum and minimum values. The impact position can be calculated by the triangulation of the Time of Flight of those points.

SHMUS can be run permanently in passive mode to detect impacts, fiber breakage in composite or any other sudden event. A subsequent test using active techniques will allow to determine whether the impact caused permanent damages on the structure.

Several test were carried out to validate the system. The results show that there is higher attenuation on signals propagating on CFRP than on aluminum. Therefore, it is required to adjust the trigger threshold level according to the type of material under test. Despite of the low energy of the impacts applied in the laboratory, the impacts were detected in both materials. Impacts on CRFP caused by a 600 gr sphere dropped from a height of 1 m were detected if the impact point was less than 30 cm away from the PWASs. Impacts on aluminum were detected from farther distance. In a real-world case, impacts capable of damaging an aircraft structure require much higher energy than those applied in the controlled environment of the laboratory and, hence, they are more likely to be detected.

Fig. 11 shows a screen capture of the demonstration video of how passive detection system works [32].

4.2. *Progressive damage detection by means of active operating mode*

The second type of tests requires not only the acquisition of signals, but also the generation of ultrasound waves to apply them to the structure under test. The SHMUS carries out both actions. Additionally, the SHMUS pre-processes the acquired data to simplify any further analysis and health diagnosis of the structure. The active damage detection was performed following two types of tests in each structure: round-robin and beamforming transmission.

Again, the echoes are acquired by all the SHMUS channels. The damage detection tests were carried out daily for two months to analyze the performance of the guided waves throughout the structures.

The initial state was set in the first day, before any damage was applied to the structure. Then, during 40 days, corrosion conditions were emulated. Saline water was added, and the aluminum and composite structures were placed together. The corrosion condition was achieved with hypertonic saline water with 2.2 % salt concentration.

There are several approaches to analyze the acquired signals. The first one consists of obtaining the degree of health matrix (DoH) according to the algorithm description given in [33,34]. Fig. 12 shows the control software screen for the SHM tests. On the first day, the test conditions are adjusted and the pristine state of the structure is defined by running ten consecutive tests. Then, each day a new round-robin test is performed and its data are compared to the pristine state. Fig. 12 shows the comparison of one hundred signals (ten

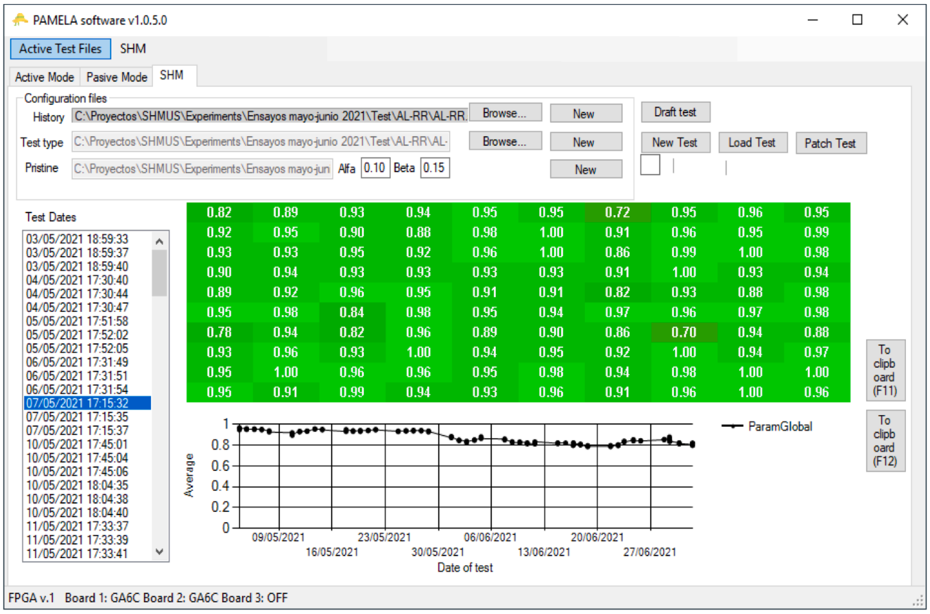

History C:\Proyectos\SHMUS\Experiments\Ensayos mayo-junio 2021\Test\AL-RR\AL-RR.

Test type C:\Proyectos\SHMUS\Experiments\Ensayos mayo-junio 2021\Test\AL-RR\AL-

Pristine C:\Proyectos\SHMUS\Experiments\Ensayos mayo-jun

Alfa 0.10 Beta 0.15

Test Dates

03/05/2021 18:59:33
03/05/2021 18:59:37
03/05/2021 18:59:40
04/05/2021 17:30:40
04/05/2021 17:30:44
04/05/2021 17:30:47
05/05/2021 17:51:58
05/05/2021 17:52:02
05/05/2021 17:52:05
06/05/2021 17:31:49
06/05/2021 17:31:51
06/05/2021 17:31:54
07/05/2021 17:15:32
07/05/2021 17:15:35
07/05/2021 17:15:37
10/05/2021 17:45:01
10/05/2021 17:45:04
10/05/2021 17:45:06
10/05/2021 18:04:35
10/05/2021 18:04:38
10/05/2021 18:04:40
11/05/2021 17:33:37
11/05/2021 17:33:39
11/05/2021 17:33:41

0.82	0.89	0.93	0.94	0.95	0.95	0.72	0.95	0.96	0.95
0.92	0.95	0.90	0.88	0.98	1.00	0.91	0.96	0.95	0.99
0.93	0.93	0.95	0.92	0.96	1.00	0.86	0.99	1.00	0.98
0.90	0.94	0.93	0.93	0.93	0.93	0.91	1.00	0.93	0.94
0.89	0.92	0.96	0.95	0.91	0.91	0.82	0.93	0.88	0.98
0.95	0.98	0.84	0.98	0.95	0.94	0.97	0.96	0.97	0.98
0.78	0.94	0.82	0.96	0.89	0.90	0.86	0.70	0.94	0.88
0.93	0.96	0.93	1.00	0.94	0.95	0.92	1.00	0.94	0.97
0.95	1.00	0.96	0.96	0.95	0.98	0.94	0.98	1.00	1.00
0.95	0.91	0.99	0.94	0.93	0.96	0.91	0.96	1.00	0.96

FPGA v.1 Board 1: GA6C Board 2: GA6C Board 3: OFF

Fig. 12. Control software for SHM active mode test on an aluminum plate with round-robin technique during two months.

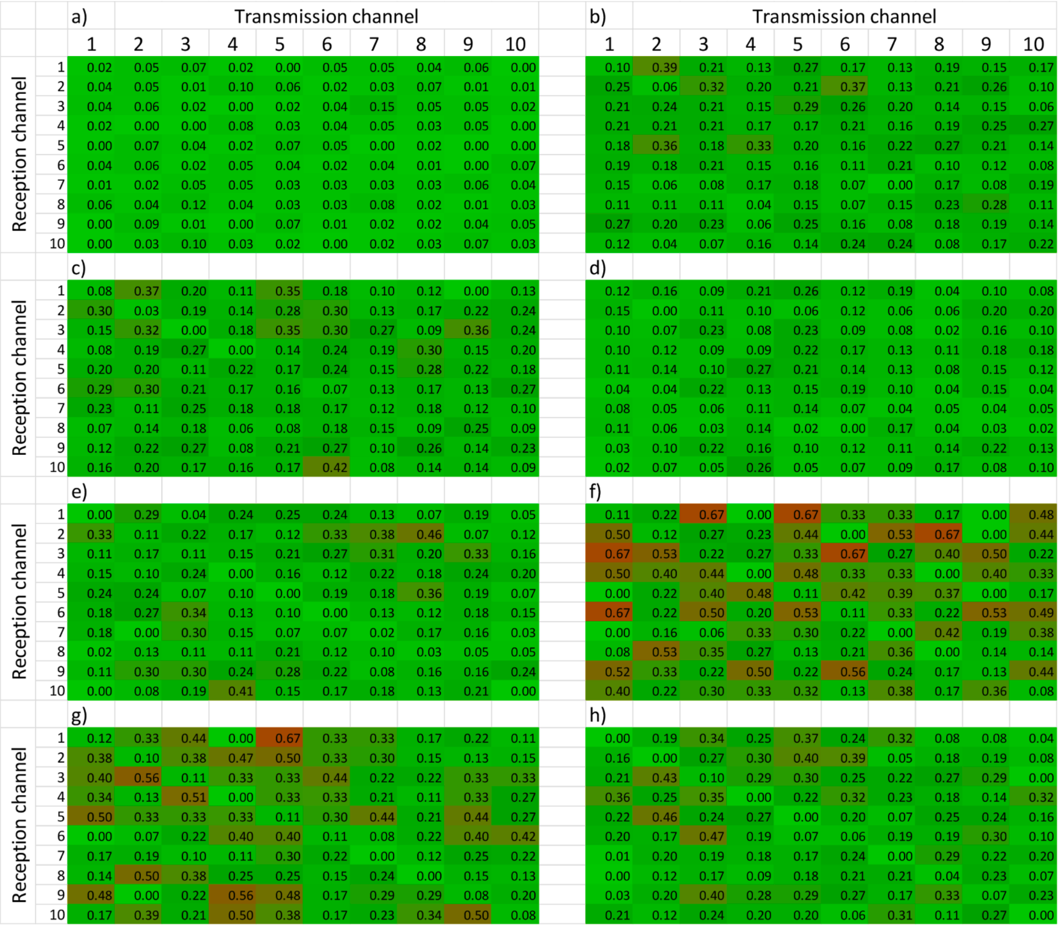

a)	Transmission channel									
	1	2	3	4	5	6	7	8	9	10
1	0.02	0.05	0.07	0.02	0.00	0.05	0.05	0.04	0.06	0.00
2	0.04	0.05	0.01	0.10	0.06	0.02	0.03	0.07	0.01	0.01
3	0.04	0.06	0.02	0.00	0.02	0.04	0.15	0.05	0.05	0.02
4	0.02	0.00	0.00	0.08	0.03	0.04	0.05	0.03	0.05	0.00
5	0.00	0.07	0.04	0.02	0.07	0.05	0.00	0.02	0.00	0.00
6	0.04	0.06	0.02	0.05	0.04	0.02	0.04	0.01	0.00	0.07
7	0.01	0.02	0.05	0.05	0.03	0.03	0.03	0.03	0.06	0.04
8	0.06	0.04	0.12	0.04	0.03	0.03	0.08	0.02	0.01	0.03
9	0.00	0.09	0.01	0.00	0.07	0.01	0.02	0.02	0.04	0.05
10	0.00	0.03	0.10	0.03	0.02	0.00	0.02	0.03	0.07	0.03

b)	Transmission channel									
	1	2	3	4	5	6	7	8	9	10
1	0.10	0.39	0.21	0.13	0.27	0.17	0.13	0.19	0.15	0.17
2	0.25	0.06	0.32	0.20	0.21	0.37	0.13	0.21	0.26	0.10
3	0.21	0.24	0.21	0.15	0.29	0.26	0.20	0.14	0.15	0.06
4	0.21	0.21	0.21	0.17	0.17	0.21	0.16	0.19	0.25	0.27
5	0.18	0.36	0.18	0.33	0.20	0.16	0.22	0.27	0.21	0.14
6	0.19	0.18	0.21	0.15	0.16	0.11	0.21	0.10	0.12	0.08
7	0.15	0.06	0.08	0.17	0.18	0.07	0.00	0.17	0.08	0.19
8	0.11	0.11	0.11	0.04	0.15	0.07	0.15	0.23	0.28	0.11
9	0.27	0.20	0.23	0.06	0.25	0.16	0.08	0.18	0.19	0.14
10	0.12	0.04	0.07	0.16	0.14	0.24	0.24	0.08	0.17	0.22

c)										
1	0.08	0.37	0.20	0.11	0.35	0.18	0.10	0.12	0.00	0.13
2	0.30	0.03	0.19	0.14	0.28	0.30	0.13	0.17	0.22	0.24
3	0.15	0.32	0.00	0.18	0.35	0.30	0.27	0.09	0.36	0.24
4	0.08	0.19	0.27	0.00	0.14	0.24	0.19	0.30	0.15	0.20
5	0.20	0.20	0.11	0.22	0.17	0.24	0.15	0.28	0.22	0.18
6	0.29	0.30	0.21	0.17	0.16	0.07	0.13	0.17	0.13	0.27
7	0.23	0.11	0.25	0.18	0.18	0.17	0.12	0.18	0.12	0.10
8	0.07	0.14	0.18	0.06	0.08	0.18	0.15	0.09	0.25	0.09
9	0.12	0.22	0.27	0.08	0.21	0.27	0.10	0.26	0.14	0.23
10	0.16	0.20	0.17	0.16	0.17	0.42	0.08	0.14	0.14	0.09

d)										
1	0.12	0.16	0.09	0.21	0.26	0.12	0.19	0.04	0.10	0.08
2	0.15	0.00	0.11	0.10	0.06	0.12	0.06	0.06	0.20	0.20
3	0.10	0.07	0.23	0.08	0.23	0.09	0.08	0.02	0.16	0.10
4	0.10	0.12	0.09	0.09	0.22	0.17	0.13	0.11	0.18	0.18
5	0.11	0.14	0.10	0.27	0.21	0.14	0.13	0.08	0.15	0.12
6	0.04	0.04	0.22	0.13	0.15	0.19	0.10	0.04	0.15	0.04
7	0.08	0.05	0.06	0.11	0.14	0.07	0.04	0.05	0.04	0.05
8	0.11	0.06	0.03	0.14	0.02	0.00	0.17	0.04	0.03	0.02
9	0.03	0.10	0.22	0.16	0.10	0.12	0.11	0.14	0.22	0.13
10	0.02	0.07	0.05	0.26	0.05	0.07	0.09	0.17	0.08	0.10

e)										
1	0.00	0.29	0.04	0.24	0.25	0.24	0.13	0.07	0.19	0.05
2	0.33	0.11	0.22	0.17	0.12	0.33	0.38	0.46	0.07	0.12
3	0.11	0.17	0.11	0.15	0.21	0.27	0.31	0.20	0.33	0.16
4	0.15	0.10	0.24	0.00	0.16	0.12	0.22	0.18	0.24	0.20
5	0.24	0.24	0.07	0.10	0.00	0.19	0.18	0.36	0.19	0.07
6	0.18	0.27	0.34	0.13	0.10	0.00	0.13	0.12	0.18	0.15
7	0.18	0.00	0.30	0.15	0.07	0.07	0.02	0.17	0.16	0.03
8	0.02	0.13	0.11	0.11	0.21	0.12	0.10	0.03	0.05	0.05
9	0.11	0.30	0.30	0.24	0.28	0.22	0.08	0.16	0.16	0.24
10	0.00	0.08	0.19	0.41	0.15	0.17	0.18	0.13	0.21	0.00

f)										
1	0.11	0.22	0.67	0.00	0.67	0.33	0.33	0.17	0.00	0.48
2	0.50	0.12	0.27	0.23	0.44	0.00	0.53	0.67	0.00	0.44
3	0.67	0.53	0.22	0.27	0.33	0.67	0.27	0.40	0.50	0.22
4	0.50	0.40	0.44	0.00	0.48	0.33	0.33	0.00	0.40	0.33
5	0.00	0.22	0.40	0.48	0.11	0.42	0.39	0.37	0.00	0.17
6	0.67	0.22	0.50	0.20	0.53	0.11	0.33	0.22	0.53	0.49
7	0.00	0.16	0.06	0.33	0.30	0.22	0.00	0.42	0.19	0.38
8	0.08	0.53	0.35	0.27	0.13	0.21	0.36	0.00	0.14	0.14
9	0.52	0.33	0.22	0.50	0.22	0.56	0.24	0.17	0.13	0.44
10	0.40	0.22	0.30	0.33	0.32	0.13	0.38	0.17	0.36	0.08

g)										
1	0.12	0.33	0.44	0.00	0.67	0.33	0.33	0.17	0.22	0.11
2	0.38	0.10	0.38	0.47	0.50	0.33	0.30	0.15	0.13	0.15
3	0.40	0.56	0.11	0.33	0.33	0.44	0.22	0.22	0.33	0.33
4	0.34	0.13	0.51	0.00	0.33	0.33	0.21	0.11	0.33	0.27
5	0.50	0.33	0.33	0.33	0.11	0.30	0.44	0.21	0.44	0.27
6	0.00	0.07	0.22	0.40	0.40	0.11	0.08	0.22	0.40	0.42
7	0.17	0.19	0.10	0.11	0.30	0.22	0.00	0.12	0.25	0.22
8	0.14	0.50	0.38	0.25	0.25	0.15	0.24	0.00	0.15	0.13
9	0.48	0.00	0.22	0.56	0.48	0.17	0.29	0.29	0.08	0.20
10	0.17	0.39	0.21	0.50	0.38	0.17	0.23	0.34	0.50	0.08

h)										
1	0.00	0.19	0.34	0.25	0.37	0.24	0.32	0.08	0.08	0.04
2	0.16	0.00	0.27	0.30	0.40	0.39	0.05	0.18	0.19	0.08
3	0.21	0.43	0.10	0.29	0.30	0.25	0.22	0.27	0.29	0.00
4	0.36	0.25	0.35	0.00	0.22	0.32	0.23	0.18	0.14	0.32
5	0.22	0.46	0.24	0.27	0.00	0.20	0.07	0.25	0.24	0.16
6	0.20	0.17	0.47	0.19	0.07	0.06	0.19	0.19	0.30	0.10
7	0.01	0.20	0.19	0.18	0.17	0.24	0.00	0.29	0.22	0.20
8	0.00	0.12	0.17	0.09	0.18	0.21	0.21	0.04	0.23	0.07
9	0.03	0.20	0.40	0.28	0.29	0.27	0.17	0.33	0.07	0.23
10	0.21	0.12	0.24	0.20	0.20	0.06	0.31	0.11	0.27	0.00

Fig. 13. DoH matrices (CFRP plate) from a) the pristine state to h) the last test day of the testing campaign.

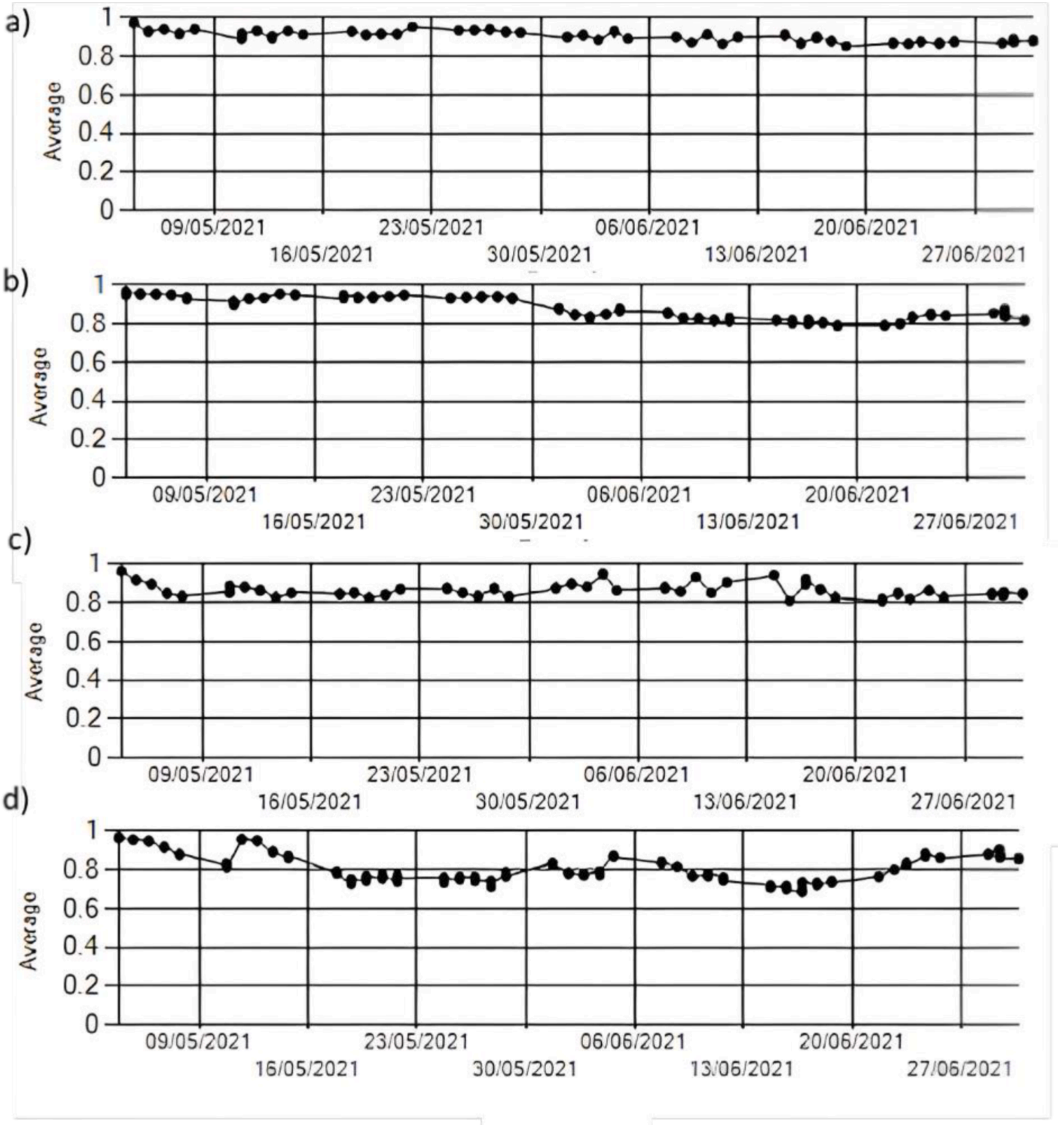

Fig. 14. Average of the DOH matrices obtained with both techniques and plates: a) Beamforming in aluminum, b) Round-robin in aluminum, c) Beamforming in CFRP, d) Round-robin in CFRP.

emissions and ten signals acquired per emission) of the current test to the pristine state. The greener and closer to '1′ a cell of the DoH matrix is, the more similar to the pristine state the health and integrity of the structure are. As the state of the structure degrades, the cell turns darker and the coefficient closer to '0′. The evolution of the average of the matrix coefficients for each performed test is shown under the colored matrix of the current test.

Fig. 13 shows the evolution of the DoH matrices over time. It only displays eight out of the 40 DoH matrices obtained after testing a CFRP plate in round-robin mode. The tests show that difference between the pristine and the actual state of the structure increases with time. Note that the DoH matrix does not depend on the type of damage considered. It helps to determine the general health state of the structure, not the localization of damage.

There is a second approach to analyze the acquired signals and assess the health state of the structure. The average of the coefficients of the DoH matrix can be calculated. Fig. 14 shows the evolution of the average during the test campaign. For both materials and methods considered, the average decreased about 20 %. It means that the pristine state of the materials is gone because of the progressive and sudden damage applied to the structures.

In fact, the colors (from green to red) of the cells of the DoH matrices, the figures in the cells, the average of the figures in each matrix, or the evolution of such average (20 % of decrease in the period analyzed in the tests), are just a dimensionless and generic number related to the test procedure. It provides an insight on the trend of the health state or the difference with respect to the pristine state.

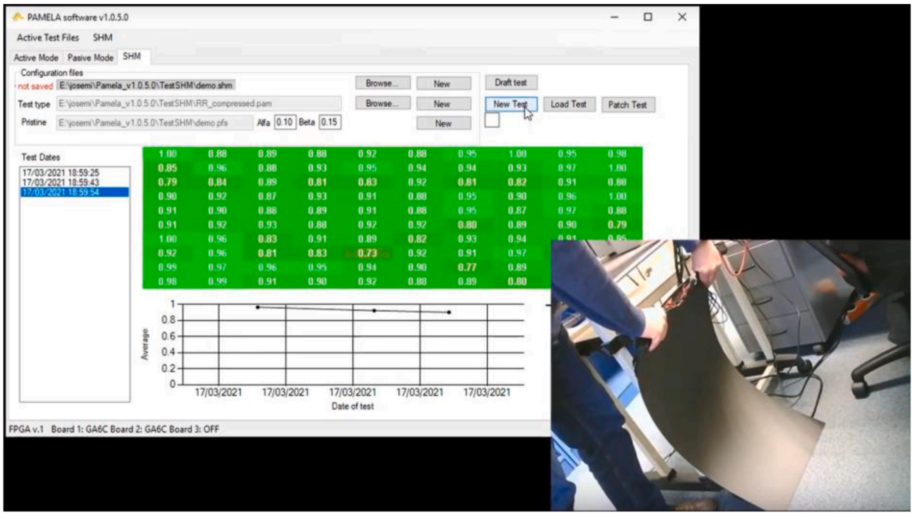

not saved E:\josemi\Pamela_v1.0.5.0\TestSHM\demo.shm

Test type E:\josemi\Pamela_v1.0.5.0\TestSHM\RR_compressed.pam

Pristine E:\josemi\Pamela_v1.0.5.0\TestSHM\demo.pfs Alfa 0.10 Beta 0.15

17/03/2021 18:59:25
17/03/2021 18:59:43
17/03/2021 18:59:54

1.00	0.88	0.89	0.88	0.92	0.88	0.95	1.00	0.95	0.98
0.85	0.96	0.88	0.93	0.95	0.94	0.94	0.93	0.97	1.00
0.79	0.84	0.89	0.81	0.83	0.92	0.81	0.82	0.91	0.88
0.90	0.92	0.87	0.93	0.91	0.88	0.95	0.90	0.96	1.00
0.91	0.90	0.86	0.89	0.91	0.88	0.95	0.87	0.97	0.88
0.91	0.92	0.93	0.88	0.92	0.92	0.80	0.89	0.90	0.79
1.00	0.96	0.83	0.91	0.89	0.82	0.93	0.94	0.91	0.95
0.92	0.96	0.81	0.83	0.73	0.92	0.91	0.97		
0.99	0.97	0.96	0.95	0.94	0.90	0.77	0.89		
0.98	0.99	0.91	0.90	0.92	0.88	0.89	0.80		

FPGA v.1 Board 1: GA6C Board 2: GA6C Board 3: OFF

Fig. 15. Screen capture of the video that shows the progressive damage detection system.

For a specific application, a calibration is necessary to relate the figure obtained from the DoH matrix to the health state of the specimen under test. Furthermore, note that the range of the number (from 1 to 0) is just a relative value in the measurement procedure. The number is not related to the deterioration of the piece of material. In any deterioration state, a new pristine state can be defined to increase the range of the number.

Detailed results of this methodology applied to fatigue crack damage can be found in [34] as well as when it is applied to corrosion in [35].

Fig. 15 exhibits a screen capture of the demonstration video of how SHMUS detects progressive damage [36].

5. Conclusions

This paper introduces a prototype intended for SHM testing, namely, an SHMUS. The prototype is based on ultrasonic techniques utilizing PWASs and it is capable of implementing both passive or AE, and active or UGWT, strategies to monitor structures. It can drive and acquire up to 18 channels simultaneously (48 channels in systems with eight input/output boards). In standard configuration, UGWT driving signals can be of 48 Vpp, but it can reach more than 100 Vpp in extended configuration.

The prototype is lightweight, small and can run several types of test according to different requirements: simple pulse-echo or pitch-catch tests, or test with multiple transducers such as round-robin, transmission beamforming, multiple delayed signal, and time reversal. It can also carry out a pre-processing stage of the acquired waveform searching for its characteristic points so that the time required to transmit the full original acquired signals is reduced.

The prototype was validated on both metallic and composite structures. The validation was carried out in passive mode for impact detection as well as in active mode for progressive damage detection.

The suitability of the SHMUS and its capability to detect low energy impacts was validated.

The methodology to perform guided-wave ultrasound tests has been detailed. Round-robin and beamforming techniques were applied to the tests as examples of active techniques.

The effects of sudden and progressive damages on the health and integrity of the structures were analyzed. The paper introduces two approaches to analyze the data from the acquired signals: DoH matrices, and average of the DoH matrices. The results show that the monitoring system SHMUS not only detects impacts and damages satisfactorily but also measures the damage as a decrease of the health of the structure under test.

In the near future, this research will continue performing new test campaigns and improving this prototype, i.e. reducing its size, weight, and adding new features, in order to improve its suitability for the aeronautical structure monitoring needs.

Declaration of Competing Interest

The authors declare that they have no known competing financial interests or personal relationships that could have appeared to influence the work reported in this paper.

Data availability

Data will be made available on request.

References

[1] S.N.A. Safri, M.T.H. Sultan, N. Yidris, F. Mustapha, Low velocity and high velocity impact test on composite materials – A review, Int. J. Eng. Sci. 3 (9) (2014) 50–60, https://doi.org/10.1177/1464420711409985.

[2] S. Gholizadeh, A review of non-destructive testing methods of composite materials, Proc. Struct. Integr. 1 (2016) 50–57, https://doi.org/10.1016/j.prostr.2016.02.008.

[3] A. Güemes, A. Fernandez-Lopez, A.R. Pozo, J. Sierra-Pérez, Structural health monitoring for advanced composite structures: A review, J. Compos. Sci. 4 (1) (2020), https://doi.org/10.3390/jcs4010013.

[4] L. Capineri, A. Bulletti, Ultrasonic Guided-Waves Sensors and Integrated Structural Health Monitoring Systems for Impact Detection and Localization: A Review, Sensors 21 (9) (Apr. 2021) 2929, https://doi.org/10.3390/s21092929.

[5] J. Gomez, J. Zubia, G. Aranguren, J. Arrue, H. Poisel, I. Saez, Comparing polymer optical fiber, fiber Bragg grating, and traditional strain gauge for aircraft structural health monitoring, Appl. Opt. 48 (8) (Mar. 2009) 1436, https://doi.org/10.1364/AO.48.001436.

[6] V. Zilberstein, et al., MWM eddy-current arrays for crack initiation and growth monitoring, Int. J. Fatigue 25 (9–11) (2003) 1147–1155, https://doi.org/10.1016/j.ijfatigue.2003.08.010.

[7] J.L. Rose, Ultrasonic Guided Waves in Solid Media, vol. 9781107048, Cambridge University Press, New York, 2014.

[8] J.P. Amezquita-Sanchez, H. Adeli, Signal Processing Techniques for Vibration-Based Health Monitoring of Smart Structures, Arch. Comput. Methods Eng. 23 (1) (Mar. 2016) 1–15, https://doi.org/10.1007/s11831-014-9135-7.

[9] H. Mei, M.F. Haider, R. Joseph, A. Migot, V. Giurgiutiu, Recent advances in piezoelectric wafer active sensors for structural health monitoring applications, Sensors (Switzerland) 19 (2) (2019) pp, https://doi.org/10.3390/s19020383.

[10] W.J. Staszewski, S. Mahzan, R. Traynor, Health monitoring of aerospace composite structures - Active and passive approach, Compos. Sci. Technol. 69 (11–12) (2009) 1678–1685, https://doi.org/10.1016/j.compscitech.2008.09.034.

[11] S. Gholizadeh, Z. Lemana, B.T.H.T. Baharudinb, A review of the application of acoustic emission technique in engineering, Struct. Eng. Mech. 54 (6) (2015) 1075–1095, https://doi.org/10.12989/sem.2015.54.6.1075.

[12] H. Kwon, Y. Park, C. Shin, J.H. Kim, C.G. Kim, Embedded silicon carbide fiber sensor network based low-velocity impact localization of composite structures, Smart Mater. Struct. 29 (5) (2020) pp, https://doi.org/10.1088/1361-665X/ab7946.

[13] G. Aranguren, J. Etxaniz, S. Cantero-Chinchilla, J.M. Gil-Garcia, M.K. Malik, Ultrasonic guided wave testing on cross-ply composite laminate: an empirical study, Sensors (Switzerland) 20 (18) (2020) 1–18, https://doi.org/10.3390/s20185291.

[14] G. Azuara, E. Barrera, M. Ruiz, D. Bekas, Damage Detection and Characterization in Composites Using a Geometric Modification of the RAPID Algorithm, IEEE Sens. J. 20 (4) (2020) 2084–2093, https://doi.org/10.1109/JSEN.2019.2950748.

[15] P. Marcus (Ed.), Corrosion Mechanisms in Theory and Practice, CRC Press, 2002, https://doi.org/10.1201/9780203909188.

[16] D. Gagar, P. Foote, P.E. Irving, Effects of loading and sample geometry on acoustic emission generation during fatigue crack growth: Implications for structural health monitoring, Int. J. Fatigue 81 (2015) 117–127, https://doi.org/10.1016/j.ijfatigue.2015.07.024.

[17] C.Q. Gómez Muñoz, F.P. García Marquez, B. Hernandez Crespo, K. Makaya, Structural health monitoring for delamination detection and location in wind turbine blades employing guided waves, Wind Energy 22 (5) (2019) 698–711, https://doi.org/10.1002/we.2316.

[18] L. Capineri, A. Bulletti, M. Calzolai, D. Francesconi, A Real-time Electronic System for Automated Impact Detection on Aircraft Structures Using Piezoelectric Transducers, Procedia Eng. 87 (2014) 1243–1246, https://doi.org/10.1016/j.proeng.2014.11.408.

[19] U. Dackermann, W.A. Smith, M.M. Alamdari, J. Li, R.B. Randall, Cepstrum-based damage identification in structures with progressive damage, Struct. Heal. Monit. 18 (1) (Jan. 2019) 87–102, https://doi.org/10.1177/1475921718804730.

[20] Q. Lei, Y. Shenfang, W. Qiang, S. Yajie, Y. Weiwei, Design and Experiment of PZT Network-based Structural Health Monitoring Scanning System, Chinese J. Aeronaut. 22 (5) (2009) 505–512, https://doi.org/10.1016/S1000-9361(08)60133-8.

[21] Physical Acoustics, "Micro-SHM — Structural Health Monitoring System," 2021. https://www.physicalacoustics.com/by-product/micro-shm-structural-health-monitoring-system/ (accessed Jan. 25, 2022).

[22] X. Tang, H. Zhao, S. Mandal, A highly-integrated CMOS transceiver for active structural health monitoring, in: 2016 IEEE National Aerospace and Electronics Conference (NAECON) and Ohio Innovation Summit (OIS), Jul. 2016, vol. 0, pp. 133–138, doi: 10.1109/NAECON.2016.7856787.

[23] Accellent, Hardware - Acellent Technologies, 2021. https://www.acellent.com/products/hardware (accessed Jan. 25, 2022).

[24] V. Dattoma, R. Nobile, F. Palano, F.W. Panella, A. Pirinu, A. Saponaro, Ultrasonic and thermographic fatigue monitoring on a full-scale CFRP aeronautical component after repairing, IOP Conf. Ser. Mater. Sci. Eng. 1038 (1) (2021) 12027, https://doi.org/10.1088/1757-899x/1038/1/012027.

[25] Z. Sharif-Khodaei, M. Ghajari, M.H. Aliabadi, A. Apicella, SMART Platform for Structural Health Monitoring of Sensorised Stiffened Composite Panels, Key Eng. Mater. 525–526 (Nov. 2012) 581–584, https://doi.org/10.4028/www.scientific.net/KEM.525-526.581.

[26] G. Aranguren, P.M. Monje, V. Cokonaj, E. Barrera, M. Ruiz, Ultrasonic wave-based structural health monitoring embedded instrument, Rev. Sci. Instrum. 84 (12) (Dec. 2013), 125106, https://doi.org/10.1063/1.4834175.

[27] S.E. Olson, M.P. DeSimio, M.M. Derriso, Beam Forming of Lamb Waves for Structural Health Monitoring, J. Vib. Acoust. 129 (6) (Dec. 2007) 730–738, https://doi.org/10.1115/1.2731404.

[28] S. Cantero-Chinchilla, G. Aranguren, M.K. Malik, J. Etxaniz, F.M. de la Escalera, An empirical study on transmission beamforming for ultrasonic guided-wave based structural health monitoring, Sensors (Switzerland) 20 (5) (2020) pp, https://doi.org/10.3390/s20051445.

[29] M. Fink, Time Reversal of Ultrasonic Fields—Part I: Basic Principles, IEEE Trans. Ultrason. Ferroelectr. Freq. Control 39 (5) (1992) 555–566, https://doi.org/10.1109/58.156174.

[30] J. Castillero, G. Aranguren, J. Etxaniz, J.M. Gil-Garcia, Composite Leading Edge Monitoring with a Guided Wave System, in: P. Rizzo, A. Milazzo (Eds.), European Workshop on Structural Health Monitoring. EWSHM 2020, Lecture Notes in Civil Engineering, 127, Springer, Cham, 2021, pp. 830–837, https://doi.org/10.1007/978-3-030-64594-6_80.

[31] J. M. Gil-García, J. Sánchez, J. Etxaniz, G. Aranguren, Demonstration video of the capabilities of the SHMUS system, YouTube, URL: https://youtu.be/DzPvJfJzMdk.

[32] J. M. Gil-García, J. Sánchez, J. Etxaniz, G. Aranguren, Demonstration video of the passive detection system, YouTube, URL: https://youtu.be/6_WymrwgWDY.

[33] S. Cantero-Chinchilla, J. Chiachío-Ruano, M. Chiachío-Ruano, J. Etxaniz, G. Aranguren, A. Jones, Y. Essa, F. Martin De La Escalera, Lamb wave-based damage indicator for plate-like structures. In Proceedings of the European Conference of the PHM Society, Utrecht, The Netherlands, 3–6 July 2018; Prognostics and Health Management Society (PHM Society): Rochester, NY, USA, 2018; Volume 4.

[34] S. Cantero-Chinchilla, G. Aranguren, J.M. Royo, M. Chiachío, J. Etxaniz, A. Calvo-Echenique, Structural health monitoring using ultrasonic guided-waves and the degree of health index, Sensors (Switzerland) 21 (3) (2021) 1–17, https://doi.org/10.3390/s21030993.

[35] G. Aranguren, J. Bilbao, J. Etxaniz, J.M. Gil-García, C. Rebollar, Methodology for Detecting Progressive Damage in Structures Using Ultrasound-Guided Waves, Sensors (Switzerland) 22 (4) (2022) pp, https://doi.org/10.3390/s22041692.

[36] J. M. Gil-García, J. Sánchez, J. Etxaniz, G. Aranguren, Demonstration video of the progressive damage detection system, YouTube, URL: https://youtu.be/hrDjFqoBNtc.